Ultrafast non-linear optical signal from a single quantum dot: exciton and biexciton effects

2004 J. Phys.: Condens. Matter 16 6185

(http://iopscience.iop.org/0953-8984/16/34/017)

INSTITUTE OF PHYSICS PUBLISHING JOURNAL OF PHYSICS: CONDENSED MATTER

J. Phys.: Condens. Matter **16** (2004) 6185–6193 PII: S0953-8984(04)80698-2

Ultrafast non-linear optical signal from a single quantum dot: exciton and biexciton effects

A Reyes[1], **F J Rodríguez**[2,3] **and L Quiroga**[2]

[1] Johannes Gutenberg-Universität Mainz, Institut für Physik, ThEP D-55099, Germany
[2] Departamento de Física, Universidad de Los Andes, AA 4976, Bogotá DC, Colombia

E-mail: frodrigu@uniandes.edu.co

Received 6 May 2004
Published 13 August 2004
Online at stacks.iop.org/JPhysCM/16/6185
doi:10.1088/0953-8984/16/34/017

Abstract

We present results on both the intensity and phase dynamics of the transient non-linear optical response of a single quantum dot (SQD). The time evolution of the four wave mixing (FWM) signal on a subpicosecond timescale is dominated by biexciton effects. In particular, for the cross-polarized excitation case a biexciton bound state is found. In this latter case, mean-field results are shown to give a poor description of the non-linear optical signal at small times. By properly treating exciton–exciton effects in an SQD, coherent oscillations in the FWM signal are clearly demonstrated. These oscillations, with a period corresponding to the inverse of the biexciton binding energy, are correlated with the phase dynamics of the system's polarization, giving clear signatures of non-Markovian effects in the ultrafast regime.

1. Introduction

Exciton dynamics experiments are attracting continuous interest because of their suitability to explore dephasing effects of single exciton and multiexciton complexes [1, 2]. Furthermore, recent proposals for solid state quantum computing systems [3–7], have stressed the importance of properly controlling multiexciton coherences. Recently, the non-classical behaviour of the light emitted from an SQD, photon antibunching in the fluorescence spectrum, has been observed in the ultrafast regime [8]. Additionally, the search for single photon sources [9] has triggered experimental interest in transient multiexciton coherences. All of these exciton based phenomena reflect the importance of interparticle interactions (electrons and holes) and their couplings to the environment, e.g., phonons. Both coherent and incoherent effects are experimentally detected. Incoherent effects are related to the system–bath interaction and from a theoretical point of view they are usually modelled within a Markov approximation.

[3] Author to whom any correspondence should be addressed.

Coherent effects are associated with multiple particle correlations and can be observed in the subpicosecond timescale. Consequently, a detailed understanding of the coherence persistence at short times is of utmost importance in nanostructure systems.

Time resolved FWM experiments give signatures of particle–particle correlations and particle–environment interactions. In a typical FWM experiment, two simultaneous excitation pulses co- or cross-circularly polarized, with wavevectors $\vec{k}_1$ and $\vec{k}_2$, propagate onto the sample. A third laser pulse, with wavevector $\vec{k}_3$, is sent time delayed at $t_2 = T$. For moderate excitation intensities, exciton–exciton interaction arises. The time evolution of the third order polarization $P^{(3)}(t, T) = |P^{(3)}(t, T)|e^{i\Phi(t,T)}$ describes the properties of the diffracted light in the $\vec{k}_3 + \vec{k}_2 - \vec{k}_1$ direction. At very short times after the excitation, particle correlations build up. These correlations have been observed using spectral interferometry techniques in bulk systems [10]. It is also possible to study the polarization phase dynamics itself, $\Phi(t, T)$. Moreover, other experiments for measuring $P^{(3)}$, like pump and probe schemes, have also been performed. In particular in [4] a simple four level model has been used to get the non-linear optical response ($\chi^{(3)}$) of an SQD. From the frequency spectrum of $\chi^{(3)}$, the possibility of getting exciton entanglement in an SQD has been predicted. However, in that work exciton correlations were included within a mean field approach (MFA).

Exciton dephasing times (T_2) have been well characterized in bulk and quantum well systems. In particular, ultrafast dynamics experiments, like time resolved speckle analysis, have been used to get dephasing time information in solids [11–13]. On the other hand, recent experiments in bulk systems show the build up of many particle correlations in the femtosecond scale of time [14]. Recently, all of these dynamical phenomena have been observed for first time in self-assembled QDs using transient FWM spectroscopy [15], where the time integrated FWM signal oscillates with the biexciton binding energy. Besides that, dephasing mechanism from optical longitudinal (LO) phonons has been observed in CdSe bulk and quantum dots systems, showing clearly non-Markovian effects associated to the coupling between carriers and LO phonons [16]. Due to its atomic-like characteristics, an SQD offers the unique possibility of manipulating the number of particles and their Coulomb interactions (exciton–exciton (X–X)) with direct consequences on decoherence processes control. Thus, rather long dephasing times ($T_2 \approx 40$ ps) have been reported [17–19].

A natural question arises when ultrafast scale of times are involved: what kind of quasiparticle (free electron–hole pairs, exciton or bound excitons) are dominant? In order to answer this question we consider the phase space filling (PSF) effect and X–X interactions on the same footing. Within MFA, the FWM signal shows contributions coming from both PSF effects as well as renormalized X–X interactions. However, this approximation fails to explain correlations at very short times. Therefore, MFA should be improved by considering quantum fluctuation effects to explain transient FWM experiments. In particular, more elaborated theoretical approaches like the one reported in [20], where a truncation in the hierarchy of polarization equations of motion to fifth order in the optical electric field is proposed, are shown to improve MFA results by including four particle correlations. Additionally, some previous reported works [20, 21] show that in bulk systems a mean-field approach to calculate the FWM signal gives errors because the exact X–X correlations are neglected.

In the present work, we go beyond previous limitations like few level systems and MFA. We use a truncation scheme similar to one developed for bulk systems [21], in which the contribution from exciton and exciton–exciton effects can be split and treated on an equal footing to any desired order in the optical field [20]. However, the truncation scheme fails to evaluate exactly the X–X Coulomb interaction due to the intensive computational work involved in its application to bulk systems. In order to get feasible results, this scheme has been used mapping the problem to a one-dimensional Hubbard model [21]. In the present

work we undertake this problem and we include exact X–X correlations in order to find the non-linear optical signal, intensity and phase dynamics in a realistic model of an SQD in the ultrafast regime. In section 2, we briefly review the theoretical background on which our results are based. Section 3 describes the main results of this work. Our conclusions are summarized in section 4.

2. Theoretical model

Our starting point is the Hamiltonian for a system of electrons and holes in a two-dimensional parabolic quantum dot excited by external laser pulses

$$\begin{aligned} H = &\sum_{\nu,s} E^{\mathrm{e}}_{\nu,s} c^{\dagger}_{\nu,s} c_{\nu,s} + \sum_{\nu,s} E^{\mathrm{h}}_{\nu,s} h^{\dagger}_{\nu,s} h_{\nu,s} \\ &+ \sum_{\nu,\sigma(s,s')} \mu^{\mathrm{eh}}_{\nu,\sigma} \mathcal{E}(t) c^{\dagger}_{\nu,s} h^{\dagger}_{\nu,s'} + \sum_{\nu,\sigma(s,s')} \mu^{\mathrm{he}}_{\nu,\sigma} \mathcal{E}(t)^{*} h_{\nu,s'} c_{\nu,s} \\ &- \sum_{\substack{\nu_1,\nu_2,\\ \nu_3,\nu_4}} \sum_{s,s'} \langle \nu_1, \nu_2 | V_{\mathrm{e-h}} | \nu_3, \nu_4 \rangle c^{\dagger}_{\nu_1,s} h^{\dagger}_{\nu_2,s'} h_{\nu_3,s'} c_{\nu_4,s} \\ &+ \tfrac{1}{2} \sum_{\substack{\nu_1,\nu_2,\\ \nu_3,\nu_4}} \sum_{s,s'} \langle \nu_1, \nu_2 | V_{\mathrm{e-e}} | \nu_3, \nu_4 \rangle c^{\dagger}_{\nu_1,s} c^{\dagger}_{\nu_2,s'} c_{\nu_3,s'} c_{\nu_4,s} \\ &+ \tfrac{1}{2} \sum_{\substack{\nu_1,\nu_2,\\ \nu_3,\nu_4}} \sum_{s,s'} \langle \nu_1, \nu_2 | V_{\mathrm{h-h}} | \nu_3, \nu_4 \rangle h^{\dagger}_{\nu_1,s} h^{\dagger}_{\nu_2,s'} h_{\nu_3,s'} h_{\nu_4,s} \end{aligned} \tag{1}$$

where $c(h)^{\dagger}_{\nu,s}, c(h)_{\nu,s}$ creates and destroys one electron (hole) in the state ν (labelled by quantum numbers $(n_{\mathrm{e(h)}}, m_{\mathrm{e(h)}})$) with spin s ($\uparrow$, spin up, $\downarrow$, spin-down). $V_{\mathrm{e-e}}$, $V_{\mathrm{e-h}}$ and $V_{\mathrm{h-h}}$, denote electron–electron, electron–hole and hole–hole Coulomb interactions, respectively. Single particle energies for electrons (holes) are given by $E^{\mathrm{e(h)}}_{\nu,s} = (n_{\mathrm{e(h)}} + m_{\mathrm{e(h)}} + 1)\omega_{\mathrm{e(h)}}$, with confinement energies $\omega_{\mathrm{e(h)}} = 1/m_{\mathrm{e(h)}} l^2_{\mathrm{e(h)}}$ ($\hbar = 1$), where $l_{\mathrm{e(h)}}$ is the parabolic confinement length size of the electron (hole). The set of laser pulses used to excite the SQD is described by the envelope amplitude $\mathcal{E}(t)$ and associated dipole moments $\mu^{\mathrm{eh}}_{\nu,\sigma}$ which take into account pulse polarizations. The spins of the electron (s) and hole (s') determine the corresponding polarization index σ, i.e., $\sigma = \sigma(s, s')$. By diagonalizing the time independent part of the Hamiltonian equation (1) ($\mathcal{E}(t) = 0$), the energies and wavefunctions for one and two excitons in an SQD are obtained, from which the non-linear optical response is calculated.

Exciton and biexciton wavefunctions are given respectively, in terms of non-interacting electron–hole pairs, as

$$\begin{aligned} |n\rangle^{\mathrm{X}}_{s,s'} &= \sum_{\nu_1,\nu_2} \Psi^{n}_{\nu_1,\nu_2} (c^{\dagger}_{\nu_1,s} h^{\dagger}_{\nu_2,s'}) |0\rangle \\ |m\rangle^{\mathrm{XX}} &= \sum_{\substack{\nu_1,\nu_2,\\ \nu_3,\nu_4}} \Psi^{m}_{\nu_1,\nu_2,\nu_3,\nu_4} (c^{\dagger}_{\nu_1,\uparrow} c^{\dagger}_{\nu_2,\downarrow} \pm c^{\dagger}_{\nu_1,\downarrow} c^{\dagger}_{\nu_2,\uparrow}) (h^{\dagger}_{\nu_3,\uparrow} h^{\dagger}_{\nu_4,\downarrow} \pm h^{\dagger}_{\nu_3,\downarrow} h^{\dagger}_{\nu_4,\uparrow}) |0\rangle. \end{aligned} \tag{2}$$

$|0\rangle$ is the SQD ground state and $\Psi^{n}_{\nu_1,\nu_2}$ and $\Psi^{m}_{\nu_1,\nu_2,\nu_3,\nu_4}$ are the exciton and biexciton amplitudes, respectively, which take properly into account the carriers' spin configuration. In the following formulae we will stick to the notation of equation (2), where the index n labels an exciton state, whereas the index m is reserved for the labelling of biexciton states.

In discussing the time resolved spectra, we will be concerned with the situation in which the SQD is excited by very short laser pulses (δ functions) in resonance with the 1s heavy-exciton state. Therefore, a large number of single particle states has to be included in the calculation of one and two exciton spectra. The applicability of the δ-pulses' limit can be extended to

typical acoustic periods when interaction with LO phonons can be neglected, compared with the deformation potential. However, it will be very important in II–VI semiconductors due to this high enough polar coupling. Our results are related with III–V systems, in which this coupling is low. In this way, when coherent phenomena coming from the oscillations of exciton or biexciton–phonon complexes are lost, incoherent phenomena acquire more importance, and after this time it is well known that a phenomenological model of decoherence, such as the one we will adopt here, can be used.

We perform our theoretical calculations following a truncation scheme [21] of the Hilbert space of one exciton and two interacting excitons. After a long algebra it is possible to give analytical expressions for the transient non-linear optical signal, which is proportional to $P^{(3)}$. It can be described as the sum of three terms: one representing the PSF (P^{PSF}) contribution, another corresponding to the MFA term (P^{MF}), and a third related to the X–X contribution (P^{F}). This last term describes exact four particle correlations and memory effects in terms of the so-called force–force time correlation function. All these terms can be calculated for an SQD described by the Hamiltonian equation (1), giving place to expressions similar but not equal to those of [21] (the differences are due to the confinement geometry of the dot; see the discussion in the next section). The resulting expressions for each one of these contributions for an SQD are given explicitly by

$$P^{\mathrm{PSF}}_{n_1,\sigma_1}(t,T)\mathrm{e}^{(\mathrm{i}\omega_{x,n_1}+\Gamma)t} = -\mathrm{i}\alpha_{n_1,\sigma_1}\sum_{\substack{n_0,n_2,n_3,\\ \sigma_0,\sigma_2,\sigma_3}} \alpha_{n_0,\sigma_0}\alpha^*_{n_2,\sigma_2}\alpha^*_{n_3,\sigma_3}\Theta(T)\Theta(t)\mathrm{e}^{(\mathrm{i}\omega_{x,n_0}-\Gamma)T}C^{n_2,\sigma_2;n_3,\sigma_3}_{n_0,\sigma_0;n_1,\sigma_1} \tag{3}$$

where $\alpha_{n,\sigma}$ is related to the exciton wavefunction at zero relative distance, $C^{n_2,\sigma_2;n_3,\sigma_3}_{n_0,\sigma_0;n_1,\sigma_1}$ is the PSF parameter (for notation details, see [21]) and $\Theta(x)$ denotes the step function ($\Theta(0)=1$). The MFA contribution can be written as

$$P^{\mathrm{MF}}_{n_1,\sigma_1}(t,T)\mathrm{e}^{(\mathrm{i}\omega_{x,n_1}+\Gamma)t} = -\mathrm{i}\alpha_{n_1,\sigma_1}\sum_{\substack{n_0,n_2,n_3,\\ \sigma_0,\sigma_2,\sigma_3}} \frac{\alpha_{n_0,\sigma_0}\alpha^*_{n_2,\sigma_2}\alpha^*_{n_3,\sigma_3}\mathrm{e}^{(\mathrm{i}\omega_{x,n_0}-\Gamma)T}\beta^{n_2,\sigma_2;n_3,\sigma_3}_{n_0,\sigma_0;n_1,\sigma_1}}{\omega_{x,n_0}+\omega_{x,n_1}-\omega_{x,n_2}-\omega_{x,n_3}+2\mathrm{i}\Gamma}$$
$$\times\ [\Theta(-T)\Theta(t+T)A_x(t,T)+\Theta(T)\Theta(t)A_x(t,0)] \tag{4}$$

where

$$\beta^{n_2,\sigma_2;n_3,\sigma_3}_{n_0,\sigma_0;n_1,\sigma_1} = \sum_m(\omega_{xx,m}-\omega_{x,n_0}-\omega_{x,n_1})B^{\sigma_0,\sigma_1}_{n_0,n_1}(m)B^{\sigma_2,\sigma_3}_{n_2,n_3}(m) \tag{5}$$

and

$$A_x(t,T) = \mathrm{e}^{(-2\Gamma+\mathrm{i}(\omega_{x,n_0}+\omega_{x,n_1}-\omega_{x,n_2}-\omega_{x,n_3}))t} - \mathrm{e}^{(2\Gamma-\mathrm{i}(\omega_{x,n_0}+\omega_{x,n_1}-\omega_{x,n_2}-\omega_{x,n_3}))T}. \tag{6}$$

Similarly, the X–X contribution is given by

$$P^{\mathrm{F}}_{n_1,\sigma_1}(t,T)\mathrm{e}^{(\mathrm{i}\omega_{x,n_1}+\Gamma)t} = \mathrm{i}\alpha_{n_1,\sigma_1}\left(\sum_m P_{n_1}(m)\right) - P^{\mathrm{MF}}_{n_1,\sigma_1}(t,T)\mathrm{e}^{(\mathrm{i}\omega_{x,n_1}+\Gamma)t} \tag{7}$$

where

$$P_{n_1}(m) = \sum_{\substack{n_0,n_2,n_3,\\ \sigma_0,\sigma_2,\sigma_3}} \alpha_{n_0,\sigma_0}\alpha^*_{n_2,\sigma_2}\alpha^*_{n_3,\sigma_3}B^{\sigma_0,\sigma_1}_{n_0,n_1}(m)B^{\sigma_2,\sigma_3}_{n_2,n_3}(m)\frac{\mathrm{e}^{(\mathrm{i}\omega_{x,n_0}-\Gamma)T}(\omega_{xx,m}-\omega_{x,n_0}-\omega_{x,n_1})}{\omega_{xx,m}-\omega_{x,n_0}-\omega_{x,n_1}-\mathrm{i}\Gamma_{xx}}$$
$$\times\ [\Theta(-T)\Theta(t+T)A_{xx}(t,T)+\Theta(T)\Theta(t)A_{xx}(t,0)] \tag{8}$$

with

$$A_{xx}(t,T) = \mathrm{e}^{(-\Gamma_{xx}+\mathrm{i}(\omega_{x,n_0}+\omega_{x,n_1}-\omega_{xx,m}))t} - \mathrm{e}^{(\Gamma_{xx}-\mathrm{i}(\omega_{x,n_0}+\omega_{x,n_1}-\omega_{xx,m}))T}. \tag{9}$$

In equations (5) and (7), m runs over all (bound and unbound) biexciton states. Bound biexcitonic states are those for which its energy lies below two times the ground state energy of an exciton. Additionally, $\beta^{n_2,\sigma_2;n_3,\sigma_3}_{n_0,\sigma_0;n_1,\sigma_1}$ and $P_{n_1,\sigma_1}(m)$ take into account the exciton and biexciton transition weights on the signal produced by the n_1 exciton state. The exciton transition weights $B^{\sigma_i,\sigma_j}_{n_i,n_j}(m)$ are defined to be the matrix elements $\langle 0|\hat{B}_{n_i,\sigma_i}\hat{B}_{n_j,\sigma_j}|m\rangle^{\mathrm{XX}}$ of the product of two nth exciton destruction operators $\hat{B}_{n,\sigma}$ between the exciton ground state $\langle 0|$ and a biexciton state $|m\rangle^{\mathrm{XX}}$. Finally, all we need is the exciton, $\omega_{x,n}$, and biexciton, $\omega_{xx,m}$, energies and their respective wavefunctions, which can be numerically obtained to any desired precision in the SQD case. From these ingredients, the exciton transition weights can be calculated as $B_{n_0,n_1}(m) = \langle 0|\hat{B}_{n_0}\hat{B}_{n_1}|m\rangle^{\mathrm{XX}}$, where the exciton destruction operator is $\hat{B}_{n,\sigma} = \sum_{\nu_1,\nu_2}\Psi^n_{\nu_1,\nu_2}c_{\nu_1,s}h_{\nu_2,s'}$ ($\sigma = \sigma(s,s')$) and $\Psi^n_{\nu_1,\nu_2}$ is the nth exciton amplitude (cf equation (2)). One of the main results of our paper is that, in contrast to an extended system, for QDs the term $P^{\mathrm{MF}}_{n_1,\sigma_1}$ does not vanish, *even* in the case of cross-polarized (CP) excitation. If the dot confinement energies are reduced, in the CP case $P^{\mathrm{MF}}_{n_1,\sigma_1}$ decreases in magnitude, approaching zero in the limit of zero confinement (extended system). This can be seen by direct evaluation of the parameter β in equation (5), that gives information on the strength of the signal as predicted by MFA. Although the β term contains information about the renormalized biexciton energy, this term is not responsible for oscillations, and only contributes with an spectral weight given by the $B^{\sigma_i,\sigma_j}_{n_i,n_j}$ changing the intensity of the FWM signal.

The total dynamics of excitons and biexcitons comprises the MF and the exact X–X contributions. The temporal dynamics dependence of P^{MF} (apart from an exponential damping) is contained in equation (6), where only contributions from differences of exciton energy levels appear, which are negligible in the case of resonant excitation. On the other hand, the temporal dependence of the X–X contribution is dominated by energy differences between two exciton states and one biexciton state, e.g. equation (9). In particular, in the CP case, a bound biexcitonic state is present, causing oscillations in the signal with a frequency corresponding to the energy of the bound state.

Exciton and biexciton dephasing rates associated to non-radiative mechanisms are described (phenomenologically) by Γ and Γ_{xx}, respectively. In the following we will concentrate only in the lowest exciton state, i.e., $n_1 = n_2 = n_3 = n_4 = 1\mathrm{s}$ with $\Gamma_{xx} = 2\Gamma$. In our model, the dephasing time T_2 is defined as the inverse of Γ_{xx}.

3. Results and discussion

In order to calculate the FWM signal for a typical self-assembled SQD [22, 23], we consider a $In_{0.5}Ga_{0.5}As$ quantum dot with $\epsilon = 12.5$, $m^*_{\mathrm{e}} = 0.068$, $m^*_{\mathrm{h}} = 0.2$, $\omega_{\mathrm{e}} = 20$ meV and $\omega_{\mathrm{h}} = 5$ meV. To guarantee a good convergence for the spectrum of zero total angular momentum excitons and biexcitons, we diagonalize a 72×72 Hamiltonian matrix for excitons and a 3250×3250 Hamiltonian matrix for biexcitons. The exciton spin is determined by the circular polarization of the excitation pulses. Further in this work we discuss only the cross polarization excitation case. With this set of parameters the biexciton binding energy is -1.27 meV.

As discussed in section 2, the FWM signal clearly depends on T, and on the exciton and biexciton energies as well as on the transition spectral weights. Excitation pulses create coherent excitons whose dephasing time (T_2) can be monitored by the delayed pulse. As the time delay increases, the FWM signal decreases, from which T_2 can be obtained. With these ingredients, and considering that more than one electronic excitation can be induced by the

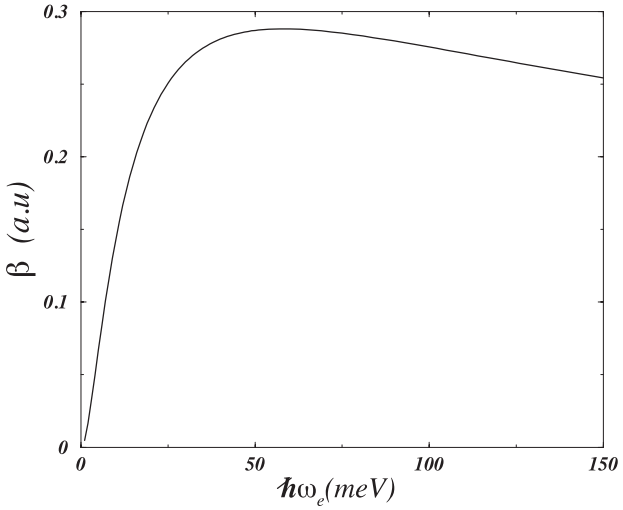

Figure 1. MFA contribution (β term) as a function of the electron and hole confinement frequencies, for $\Gamma_{xx} = 0.125$ meV.

laser and four particle correlations occur for times lesser than $T_2/4$, we expect that interference phenomena appear in the ultrafast timescale. Therefore, the coherent FWM signal and the phase dynamics give clear signatures of exciton–exciton interactions in the ultrafast regime. In the following we will not be concerned with T_2 determination, which is to be taken as a free parameter. Pulses with zero time delay, $T = 0$, will be considered.

In the weak intensity regime both PSF and X–X effects determine the non-linear optical properties. We will concentrate on these two contributions. PSF contributions to the FWM signal are only important in the parallel spin exciton case, where X–X effects are negligible, because a bound biexciton state does not exist at all. By contrast, for the cross polarization situation we are interested in, PSF effects are vanishing while X–X effects become dominant. It is important to remark that in extended and isotropic systems the MFA gives a zero contribution to the FWM signal, because only excited excitons with zero centre of mass momentum contribute, i.e., ($\vec{q} = 0$) [21]. However, in an SQD this condition can be relaxed due to the fact that the parabolic potential absorbs the incident momentum, and excitons with centre of mass momentum different from zero can be excited. This point becomes particularly clear by considering the mean field parameter β defined in equation (5). Whereas for extended systems this parameter is exactly zero [21], for an SQD it becomes a function of the confinement energies $\omega_{\mathrm{e(h)}}$. The dependence of β on ω_{e} is depicted in figure 1. We consider a constant relationship between electron and hole confinement lengths, i.e., $l_{\mathrm{e}} = l_{\mathrm{h}}$. It can be seen that in the limit of small confinement, i.e., pure two-dimensional systems ($\omega_{\mathrm{e,h}} = 0$), β tends to zero, as it should. This means that the usual condition of ($\vec{q} \neq 0$) for the carriers' Coulomb interaction in extended systems is broken in confined systems. We have tested our results taking a huge set of excitonic states and we found that higher energy states give a negligible contribution to β.

The phase dynamics and the non-linear optical signal are calculated for different decay rates. In order to better clarify why MFA is not adequate to describe non-linear optical signals at small times, we plot in figure 2, separately, the amount of particle correlation contribution to the FWM signal as described within MFA (equation (4)) and exact X–X effects (equation (7)), which include memory (non-Markovian) effects, for $\Gamma_{xx} = 0.125$ meV. The usual and simplest

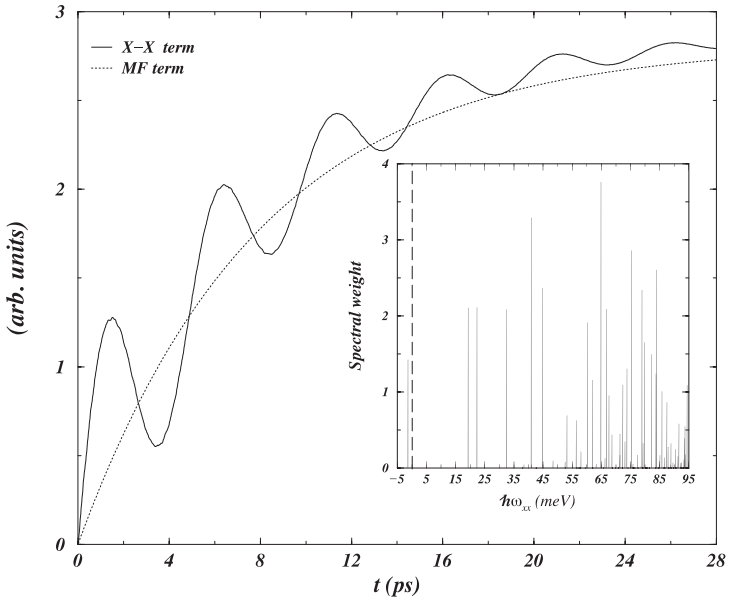

Figure 2. Absolute values of the MFA contribution (real part of $P^{\mathrm{MF}}_{n_1}(t, T)\mathrm{e}^{(\mathrm{i}\omega_{x,n_1}+\Gamma)t}$) and X–X contribution ($P^{\mathrm{F}}_{n_1}(t, T)\mathrm{e}^{(\mathrm{i}\omega_{x,n_1}+\Gamma)t}$) to the FWM signal, for $\Gamma_{xx} = 0.125$ meV. Inset: spectral weight of the biexciton wavefunction. Bound biexciton energy $= -1.27$ meV. The long-dashed curve denotes the zero energy.

approximation for this last term yields to the Markov approximation and MFA results. By contrast, in this work we have performed a full numerical evaluation of X–X effects by summing over all biexciton states. Hence, we plot the absolute values of both the real part of $P^{\mathrm{MF}}_{n_1,\sigma_1}(t, T)\mathrm{e}^{(\mathrm{i}\omega_{x,n_1}+\Gamma)t}$ (MFA term) and the real part of $P^{\mathrm{F}}_{n_1,\sigma_1}(t, T)\mathrm{e}^{(\mathrm{i}\omega_{x,n_1}+\Gamma)t}$ (X–X term). The MFA result grows monotonically with t, whereas the X–X result shows beating oscillations with a period corresponding to $T_{xx} = 2\pi\omega^{-1}_{xx,opp} \approx 5$ ps, the biexciton binding energy. As can be seen, non-Markovian effects arising from exciton–exciton correlations are the main source of discrepancies between MFA results and the exact ones. This means that ultrafast spectroscopy in SQDs should register memory effects associated to four particle correlations.

In the inset of figure 2, we show the spectral weight $B(m)$ as a function of biexciton energy levels (the zero of energy corresponds to twice the single 1s-heavy-exciton energy). We have only plotted those levels that have total angular momentum $L_z = 0$. The bound biexciton level is clearly seen at negative energies. Although unbound biexciton states have non-negligible spectral weights, the bound biexciton still has a comparable weight. As can be seen in figure 2, MFA fails to describe properly four particle interactions at very short times, where particle–particle correlations are important. This term does not oscillate and only average the exact result. Besides that, the contribution in equation (7) takes into account a higher degree of correlation going beyond MF and gives oscillations at very short times. These oscillations provide information about strong correlations between excitons. Thus, the bound biexciton dynamics is directly linked to non-Markovian effects. By contrast, in the long time limit ($t > T_2$), memory effects are lost and MFA results approach the real part of the first term in equation (7). The FWM signal becomes dominated by non-radiative dephasing effects, producing in this way a simple exponential decay.

In order to assess how the main features described above are reflected on the optical dynamical characteristics, we plot the non-linear FWM intensity $|P^{(3)}(t, 0)|$ in figures 3(a)

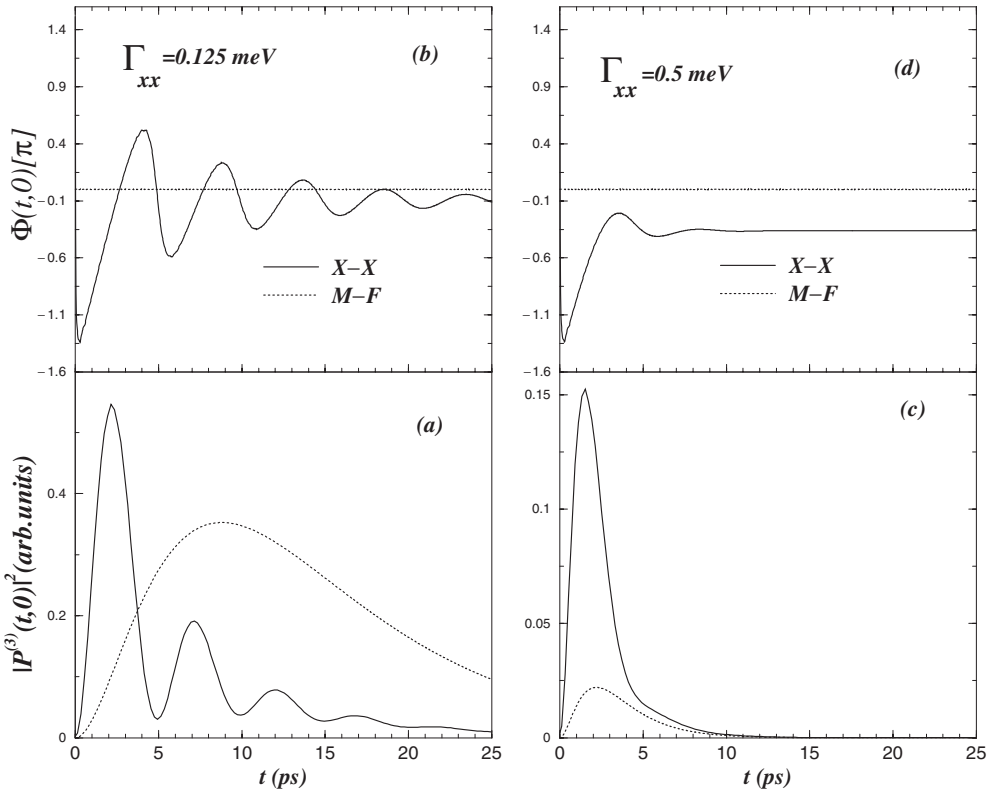

Figure 3. $\Gamma_{xx} = 0.125$ meV: (a) time resolved FWM signal; (b) phase dynamics. $\Gamma_{xx} = 0.5$ meV: (c) time resolved FWM signal; (d) phase dynamics.

and (c), and the dynamical phase $\Phi(t, 0)$ in figures 3(b) and (d), for dephasing rates $\Gamma_{xx} = T_2^{-1} = 0.125$ and 0.5 meV, respectively. To better illustrate the results, a comparison is made between MFA and X–X results on the same plots. For a low dephasing rate ($T_2 \approx 8$ ps), strong oscillations are clearly seen in figures 3(a) and (b) for $t < T_2$. The X–X interaction induces a π phase shift with respect to the incident electric field. The phase of the $P^{(3)}$ signal oscillates during a typical time T_2. The FWM signal shows a strong peak at $t \approx T_2/4$ whereas it should have a maximum at $t \approx T_2$ from MFA. For high dephasing rates ($T_2 \approx 2$ ps), figures 3(c) and (d), the attenuation of both the intensity and phase of the third order optical signal is evident. At this timescale, the T_2 dephasing time is shorter than the time for which coherent effects could be seen. It is worth noting that while the phase shows a similar starting behaviour as compared with the low dephasing case, the FWM signal intensity is drastically reduced by roughly a factor of five (notice the change of vertical scale).

Most importantly, the phase dynamics exhibits novel features at small times when exciton–exciton correlations are considered. By contrast, MFA results yield to a real $P^{(3)}$ for any time. Therefore, no phase dynamics is observed within MFA. In particular, X–X effects present a correlation between the first FWM signal minimum and a π jump in its phase. For long times the phase goes to a constant value. However, after the extinction of the FWM intensity, there is no longer a clear physical meaning for this phase. Hence, oscillations in the phase dynamics, with a beating frequency controlled by the biexciton binding energy, could bring important information about exciton correlations in SQDs. In contrast with higher dimensional systems

(quantum wells and bulk samples), an SQD provides us with an adequate system where exciton and biexciton discrete energy spectra can be tailored by changing the confinement potential. In this way, optimal conditions to enhance phase memory could be explored.

4. Conclusions

In summary, we have studied the non-linear optical response from multiexciton complexes in an SQD. For cross-polarized excitation, the creation of bound biexcitons is possible. They dominate the non-linear polarization dynamics in the low density regime. The phase dynamics and the FWM signal in the ultrafast scale of time have been obtained. By including all the numerically determined biexciton states, exact exciton–exciton correlations are evaluated allowing to go beyond simple MFA results. In particular we found that the phase dynamics and the FWM intensity oscillate with a period which coincides with the inverse of the bound biexciton frequency. We demonstrated clearly that the usual mean field theory, which is closely related to the Markovian approximation, does not describe correctly exciton correlations at very small times. However, our results show that at long times, MFA results for both intensity and phase dynamics are close to those produced by a more realistic calculation.

Acknowledgments

FJR and LQ acknowledge partial support from COLCIENCIAS (Colombia) project No. 1204-05-10326/11408, Banco de la República (Colombia) and from the EPSRC-DTI LINK project (UK).

References

[1] Bonadeo N H *et al* 1998 *Phys. Rev. Lett.* **81** 2759
[2] Regelman D V *et al* 2001 *Phys. Rev. Lett.* **87** 257401
[3] Quiroga L *et al* 1999 *Phys. Rev. Lett.* **83** 2270
[4] Chen G *et al* 2000 *Science* **289** 1906
[5] Bayer M *et al* 2001 *Science* **291** 451
[6] Piermarochi C *et al* 2002 *Phys. Rev.* B **65** 075307
[7] Hohenester U, Rossi F and Molinari E 1999 *Physica* B **272** 1
[8] Becher C *et al* 2001 *Phys. Rev.* B **63** 121312
[9] Moreau E *et al* 2001 *Phys. Rev. Lett.* **87** 183601
[10] Lepetit L *et al* 1995 *J. Opt. Soc. Am.* **12** 2467
[11] Feuerbacher B F *et al* 1991 *Phys. Rev.* B **43** 2439
[12] Bigot J-Y *et al* 1993 *Phys. Rev. Lett.* **70** 3307
[13] Langbein W *et al* 1999 *Phys. Rev. Lett.* **82** 1040
[14] Huber R *et al* 2001 *Nature* **414** 286
[15] Borri P *et al* 2001 *Phys. Rev. Lett.* **87** 157401
[16] Woggon U *et al* 2001 *Phys. Rev.* B **61** 1935
[17] Kamada H *et al* 2001 *Phys. Rev. Lett.* **87** 246401
[18] Bacher G *et al* 1999 *Phys. Rev. Lett.* **83** 4417
[19] Zwiller V *et al* 1999 *Phys. Rev.* B **59** 5021
[20] Axt V M *et al* 1994 *Z. Phys.* B **93** 195
[21] Östreich Th *et al* 1998 *Phys. Rev.* B **58** 12920
[22] Raymond S *et al* 1997 *Superlatt. Microstruct.* **21** 541
[23] Wojs A *et al* 1995 *Phys. Rev.* B **51** 10880